HIGH POWER LASER
SCIENCE AND ENGINEERING

RESEARCH ARTICLE

High-repetition-rate and high-power efficient picosecond thin-disk regenerative amplifier

Sizhi Xu[1], Yubo Gao[1], Xing Liu[1], Yewang Chen[1], Deqin Ouyang[1], Junqing Zhao[1], Minqiu Liu[1],
Xu Wu[1], Chunyu Guo[3], Cangtao Zhou[4], Qitao Lue[2], and Shuangchen Ruan[1]

[1] *Key Laboratory of Advanced Optical Precision Manufacturing Technology of Guangdong Higher Education Institutes, Sino-German College of Intelligent Manufacturing, Shenzhen Technology University, Shenzhen, China*

[2] *Han's Laser Technology Industry Group Co., Ltd., Shenzhen, China*

[3] *Shenzhen Key Laboratory of Laser Engineering, College of Physics and Optoelectronic Engineering, Shenzhen University, Shenzhen, China*

[4] *Shenzhen Key Laboratory of Ultraintense Laser and Advanced Material Technology, College of Engineering Physics, Shenzhen Technology University, Shenzhen, China*

Abstract

We present an effective approach to realize a highly efficient, high-power and chirped pulse amplification-free ultrafast ytterbium-doped yttrium aluminum garnet thin-disk regenerative amplifier pumped by a zero-phonon line 969 nm laser diode. The amplifier delivers an output power exceeding 154 W at a pulse repetition rate of 1 MHz with custom-designed 48 pump passes. The exceptional thermal management on the thin disk through high-quality bonding, efficient heat dissipation and a fully locked spectrum collectively contributes to achieving a remarkable optical-to-optical efficiency of 61% and a near-diffraction-limit beam quality with an M^2 factor of 1.06. To the best of our knowledge, this represents the highest conversion efficiency reported in ultrafast thin-disk regenerative amplifiers. Furthermore, the amplifier operates at room temperature and exhibits exceptional stability, with root mean square stability of less than 0.33%. This study significantly represents advances in the field of laser amplification systems, particularly in terms of efficiency and average power. This advantageous combination of high efficiency and diffraction limitation positions the thin-disk regenerative amplifier as a promising solution for a wide range of scientific and industrial applications.

Keywords: high efficiency; high power; picosecond laser; regenerative amplifier; thin-disk laser

1. Introduction

In the realm of ultrafast technology, high-repetition-rate, efficient and high-power laser sources are essential in a wide range of applications. Their profound impact is evident in a variety of fields, particularly in spectroscopy[1,2], materials processing[3,4] and laser micromachining[5,6] and there are consistent pushes for the development of more reliable, efficient laser sources.

As the demand for enhanced performance in laser systems continues to grow, traditional rod-type solid-state lasers have faced inherent limitations. These limitations include challenges related to thermal management, beam quality and scalability to higher power levels. Researchers have made significant advancements in laser technology to overcome these challenges, resulting in the development of more efficient and sophisticated laser architectures. Notably, fiber master oscillator power amplifiers[7,8], slab lasers[9,10] and thin-disk lasers (TDLs)[11–13] have emerged as noteworthy solutions, each of which offers a high surface-to-volume ratio for effective heat extraction. Among them, the TDL, with a thickness of sub-mm, stands out for its superior energy storage capacity and efficient 1D heat dissipation. These inherent advantages enable the TDL to achieve outstanding performance metrics, such as generating kW-level average power without chirped pulse amplification (CPA), producing a picosecond (ps) pulse energy at the mJ level, and achieving a peak power exceeding 1 GW[14–16]. Recent strides in this technology have marked significant milestones, with pulse energies reaching an impressive 720 mJ at a repetition rate of 1 kHz[17]. These

Table 1. Summary of published results from thin-disk regenerative amplifiers.

Av. power (W)	PRF/kHz	Pulse width (ps)	M^2	Pump power	Opt-opt eff.	Ref.
0.12	1	2.3	/	8 W@940 nm	1.5%	[18]
75	3	1.6	1.1	284 W@940 nm	26.4%	[24]
24	0.1	1.8	1.04	133 W@940 nm	18.0%	[25]
126	200	800	1.42	1.2 kW@940 nm	10.5%	[26]
56	200	0.534	1.24	150 W@969 nm	37.3%	[27]
550	92	2	1.4	1.25 kW@969 nm	44.0%	[20]
1950	20	0.8	/	4.5 kW@969 nm	43.3%	[23]
150	1000	6	<1.3	330 W@969 nm	45.4%	[28]
154	1000	6.82	1.06	260 W@969 nm	61.0%	This work

Note: Av. power, average power; PRF, pulse repetition frequency; opt-opt eff., optical–optical conversion efficiency.

breakthroughs signify substantial progress in ytterbium-doped yttrium aluminum garnet (Yb:YAG)-based TDLs, leading to notable improvements in various performance aspects, such as enhanced optical efficiency and reduced quantum defect and heat load.

In thin-disk geometry, the short pump beam path inside the active medium causes low pump absorption efficiency, which can lead to a decrease in overall optical efficiency. Thus, a multi-pass pump beam configuration through the thin disk is required for an efficient laser operation. The concept of a thin-disk regenerative amplifier was first introduced by A. Giesen et al.[18] in 1997 and achieved an output power of 0.12 W. Here, they utilized only an eight-pump pass configuration in a 300-μm thick disk, which results in a low optical-to-optical efficiency of 1.5%. To address this limitation, a common approach is to employ a multi-pass imaging configuration, redirecting the unabsorbed pump light back into the active medium[19]. This technique significantly enhances pump absorption, thereby improving the optical efficiency of the TDL system. Smrz et al.[20] reported on the PERLA C laser system, which demonstrated a high-power output of 550 W at a pumping power of 1250 W, achieving an optical-to-optical conversion efficiency of 44%. Typically, Yb:YAG-based TDLs are pumped at a wide absorption band around 940 nm, resulting in a quantum defect of 8.7% when lasing at 1030 nm[21]. However, it is possible to further reduce the quantum defect to 5.8% by pumping the laser at around 970 nm. This shift in pumping wavelength decreases the heat load by more than one-third, which can significantly improve the overall performance of the laser system. Although Yb:YAG crystals offer advantages for high-power lasers, their narrow absorption band (~2 nm) at 969 nm poses a challenge due to the possible shift in laser diode (LD) wavelength at high power. However, high-power wavelength-stabilized LDs utilizing volume Bragg gratings (VBGs) have enabled the implementation of 'zero-phonon line' (ZPL) pumping at 969 nm, even in high-power systems. This approach allows efficient energy absorption and utilization in the TDL system[22]. As a result of these advancements, the output power of the regenerative amplifier has been successfully expanded to 1.95 kW, with a pumping power of 4.5 kW, achieving an impressive optical-to-optical

conversion efficiency of 43.3%[23]. These developments represent substantial advancements in enhancing the performance of high-power TDL systems, making them viable for various applications.

However, the optical-to-optical conversion efficiencies of current thin-disk regenerative amplifiers remain below 50%[24–28], as shown in Table 1. Hence, it is imperative to develop a thin-disk regenerative amplifier with high optical conversion efficiency to meet the stringent demands of ultrafast laser applications effectively.

In this paper, we present a significant improvement in ultrafast thin-disk regenerative amplifiers, achieving the highest optical efficiency to date. We achieved an exceptional optical conversion efficiency of 61%, surpassing previous reports by more than 15%, by employing custom-designed 48 passes in a Yb:YAG thin-disk regenerative amplifier pumped by a ZPL 969 nm LD. This efficiency was achieved by using ZPL pumping with a fully locked spectrum, ensuring precise control over the amplification process. The experimental findings exhibit exceptional results as the amplifier achieved 154 W of output power at 1 MHz, thereby highlighting its robust high-power capabilities. The outstanding results stem from the synergy among a high-quality thin-disk crystal, an effective heat-sink encapsulation, a high-absorption pump system and a well-designed cavity. This complementary combination of efforts promoted the efficient, high-quality and stable output of the thin-disk regenerative amplification system. The achieved optical-to-optical efficiency of 61% signifies a noteworthy progress in ultrafast thin-disk regenerative amplifiers, overcoming previous limitations and unveiling new possibilities for ultrafast laser applications.

2. Thin-disk regenerative amplifier

2.1. Experiment setup

The experimental setup of the high-power efficient picosecond TDL is illustrated in Figure 1. The major components of the system included a fiber seed oscillator, a TDL head and a regenerative cavity. The regenerative amplifier was designed with an optimized cavity, eliminating the need for common
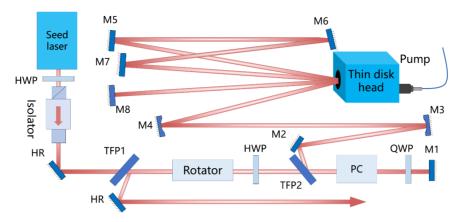
Figure 1. Optical scheme of the regenerative amplifier. HWP, half-wave plate; QWP, quarter-wave plate; TFP1, TFP2, thin film polarizer; PC, Pockels cell; M1, M2, M5–M8, mirror; M3, M4, concave mirror.

ultrafast amplifier components such as seed selection, pre-amplification and a CPA structure. To amplify the energy of 1030 nm seed pulses, we employed an all-fiber oscillator mode-locked by a semiconductor saturable absorber mirror (SESAM) with a pulse duration of 7.1 ps at a repetition rate of 30 MHz, serving as the seed for the subsequent amplification in the regenerative amplifier. The average power of the seed laser was 15 mW, corresponding to a pulse energy of 0.5 nJ. The regenerative cavity consisted of a Pockels cell (PC), thin film polarizers (TFPs), quarter-wave plates (QWPs) and a carefully designed resonant cavity. An isolator after the seed laser was used to prevent undesirable feedback of the amplifier from damaging the setup. Subsequently, an additional isolator structure consisting of a TFP, a rotator and a half-wave plate was arrayed to separate the input and output pulses. The p-polarized pulses from the seed laser were directed into the regenerative amplifier through TFP2. A periodic high voltage was applied to the PC to selectively trap pulses that had passed through the PC twice and were propagating within the regenerative cavity. The cavity period needs to be precisely controlled, being lower than the time interval between successive output pulses while higher than the rise or fall time of the PC voltage. Thereafter, only the desired pulse oscillated within the cavity, undergoing efficient amplification during roundtrip propagation, while other pulses escaped from the cavity directly because of their undesirable temporal characteristics.

A Yb:YAG thin disk, doped at a concentration of 9% (atomic fraction), with a diameter of 8.8 mm and a thickness of 150 μm, was used as the active medium. Our thermal management system is thoughtfully designed, integrating highly efficient impingement cooling techniques and precise bonding to a high thermal conductivity diamond substrate. These advanced features synergistically work together to ensure optimal performance, reliability and efficiency of the thin-disk regenerative amplifier. The front face of the Yb:YAG disk was coated for anti-reflectivity (AR), while the back face was coated for high reflectivity (HR) at 969

and 1030 nm. Due to the thinness of the disk, the absorption of the pump power after a single pass was limited to a small percentage, approximately 6%. To maximize pump absorption and protect the LD, we employed a 48-pass pump structure, as depicted in Figure 2(a), consisting of two reflective prisms and a parabolic mirror, resulting in a power extraction efficiency exceeding 95%. Meanwhile, we substituted the 940 nm pump with a ZPL pump at 969 nm, resulting in a quantum defect from 8.7% to 5.8%. The high-power top-hat pump diode with a maximum power of 260 W was focused onto the disk by a collimating lens and the parabolic mirror using a spot diameter of 2.3 mm, which corresponds to a power density of 6.26 kW/cm^2. The regenerative resonator consisted of a telescope structure (M3, M4) and several plane mirrors (M1, M2, M5–M8) to ensure precise mode matching among the seed laser, pump laser and resonator. Various polarized elements, such as the PC, TFP2 and HWP, were incorporated into the setup to maintain the amplification during roundtrip propagation. All the cavity mirrors (M1–M8) were highly reflective at 1030 nm at 0°. M3 and M4 were concave mirrors with a curvature radius ratio of 500:700. Moreover, the pulse experienced four reflections from the thin disk per roundtrip, which indicates eight passes through the Yb:YAG disk.

The propagation modes on the sagittal and tangential faces of the regenerative cavity simulated by the Gaussian propagation matrix are shown in Figure 2(b). The length of the regenerative amplifier was 2.5 m, with the fundamental mode diameters measuring 1.8, 1.3 and 1.4 mm at the disk, PC and TFP2, respectively. Only the TEM$_{00}$ laser was supported for the cavity design due to relatively large mode diameters at the disk and PC locations. It ensured a diffraction-limited beam, substantially improving the spatial property of the output laser. In addition, large spots reduced the power density from the pump and amplified pulses, mitigating the risk of crystal damage without a CPA structure. The sufficiently large fundamental mode on the disk and PC corresponded to the maximum peak power densities of
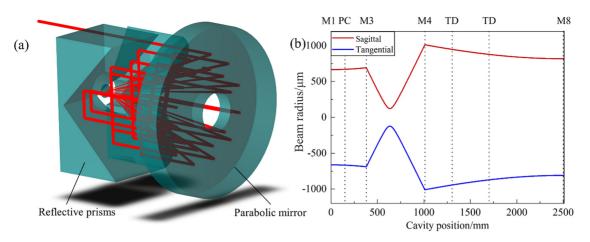
Figure 2. Thin-disk laser systems: (a) 48-pass pump system and (b) beam radius of the regenerative cavity.

Table 2. Thermo-mechanical properties of materials for the FEM[31].

Material	Thermal conductivity (W/(m K))	Coefficient of thermal expansion (K^{-1})	Density (kg/m^3)	Coolant temperature (K)
Yb:YAG	6.5	6.3×10^{-6}	4776.6	
Diamond	1800	1×10^{-6}	3515.0	300
Copper	388	1.7×10^{-5}	8936.8	

1.77 and 3.4 GW/cm^2 (154 W, 500 kHz), respectively, which were below the damage thresholds of the crystal[29,30].

2.2. Results and discussion

In order to achieve an efficient and high-quality laser, ingenious optimization of the cooling structure for the thin-disk crystal is indispensable. This approach reduces wavefront distortion caused by the active medium, and reduces thermal deformation of the thin disk, ensuring the stability of the regenerative cavity. For analyzing the effectiveness of the cooling system, a numerical finite element method (FEM) is applied to solve the 3D steady-state heat-conduction problem. The geometric and thermo-mechanical properties of the Yb:YAG and diamond heat sink at 300 K are detailed in Table 2. As the Yb:YAG directly interacts with the laser, its thermal conductivity should be treated as a temperature-dependent value[31]. We assumed that the size and structure of both the thin disk and diamond matched with the experiment, and copper was used for the cooling components. The cooling system was modeled through the finite element commercial COMSOL Multiphysics. A notable advantage of COMSOL is its multi-physics coupling, allowing efficient simulation for the impingement cooling and temperature distribution within the module.

The left panel in Figure 3(a) illustrates the mesh structure of the model, which is divided into free tetrahedra. We simulated the water flow with turbulence, using an inlet of 10 mm and a water velocity of 1 m/s. It cooled the backside of the diamond substrate through an array of 1.5 mm diameter holes, as shown in the lower right panel

of Figure 3(a). The upper right panel of Figure 3(a) displays the spatial distribution of the flow velocity. It is observed that the water flow is homogeneous and fast around the diamond, indicating efficient heat dissipation. Furthermore, we coupled the heat transfer in the solids physical field. The temperature distribution for the cooling system model, including the crystal and diamond heat sink at a pumping power of 260 W, is shown in Figure 3(b). It indicates that the cooling structure effectively mitigates the thermal accumulation effects. For a pump intensity of 6.26 kW/cm^2, the thin-disk crystal operates at a stable temperature of 60°C. This controlled temperature within the system is conducive to the efficient and stable operation of high-power lasers.

For the experiment, the top-hat beam profile homogenizes the energy distribution of the pump on the disk, effectively mitigating temperature variations and beam distortion. Compared to the Gaussian-distributed pump, the pump scheme with the top-hat imaging significantly reduces the thermal lensing. This method diminishes the aspherical wavefront distortions caused by uneven heat distribution within the disk and reduces losses from the phase aberration. In addition, it provides a more uniform thermal stress distribution across the pump module, promoting the stability of the laser system[32,33]. As a result, the regenerative amplifier achieves a more stable and efficient single-mode output. The pump profile and normalized line-out are shown in Figures 4(a) and 4(b), respectively, illustrating a uniform distribution of the pump on the disk surface with a full width at half maximum (FWHM) of 2.3 mm. Furthermore, the temperature distribution at the disk at various powers was investigated by an infrared thermal camera (T1010, FLIR) on our system while the regenerative amplifier
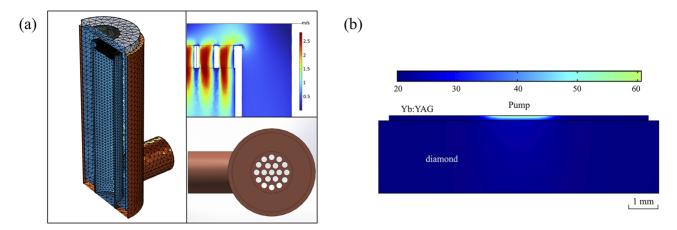
Figure 3. FEM model for thin-disk Yb:YAG. (a) Mesh model and structure of the cooling system. (b) Temperature distribution.
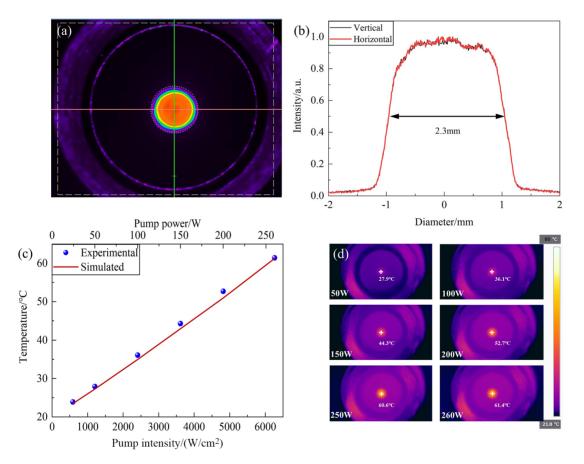

Figure 4. Pump spot on the disk. (a) Pump profile. (b) Line-out. (c) Temperature distribution versus pump intensity. (d) Image from an infrared thermal camera.

was operating, as shown in Figure 4(c). The temperature on the disk shows a near-linear increase with increasing pump power. The FEM results for the 969 nm LD are represented by the red solid line. The experimental and simulated results exhibit a strong correspondence. As depicted in Figure 4(d), the temperature distribution details indicate that the thin-disk crystal experiences a comparatively gradual temperature increase during its operation phase. At the maximum pump

power of 260 W, the highest temperature at the disk was only 61.4°C, with relatively small localized temperature differences, indicating that the thermal management of our pump system was effective.

As depicted in Figure 5(a), the output average power at 1030 nm increases with the increase in pump power for the regenerative amplifier at 1 MHz. We obtained the maximum output power of 154.1 W after 50 roundtrips of the
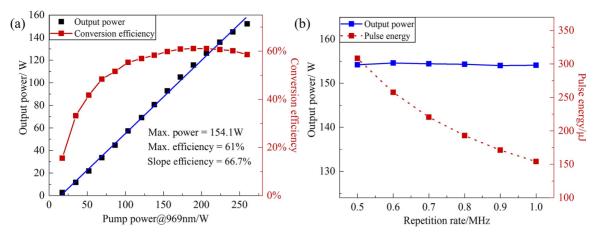
Figure 5. Power characteristics of the thin-disk regenerative amplifier. (a) Pump power versus output power and efficiency at 1 MHz. (b) Average power and pulse energy at the maximum power versus repetition rate.
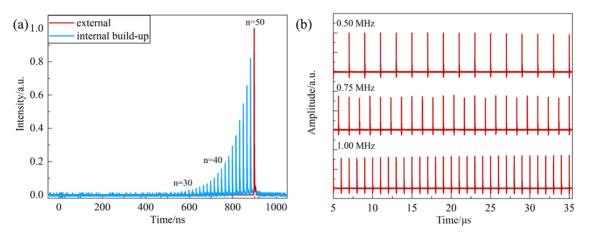

Figure 6. Temporal characteristics of the thin-disk regenerative amplifier. (a) Intracavity pulse build-up; n, number of roundtrips. (b) Temporal pulse trains.

amplification with a pump power of 260 W, corresponding to a conversion efficiency of 59.3%. However, we obtained the maximum conversion efficiency of 61% with the pump power of 200 W. A slight decrease in efficiency from 61% to 59.3% was observed when the pump power increased from 200 to 260 W, which was attributed to the gain saturation at 200 W. With appropriate modulation of the PC gate frequency, we investigated the output characteristics, including average output power and pulse energy, at repetition rates from 0.5 to 1 MHz, as depicted in Figure 5(b). During the amplification phases at all repetition rates, the pulses consistently underwent 200 times of reflection at the disk. As the repetition rate increased, the maximum average output power remained at 154 W without significant changes. Thereby, the pulse energy and pulse peak power presented declining trends. At the minimum repetition rate of 0.5 MHz, a maximum pulse energy of 308 µJ and a maximum peak power of 45 MW were obtained.

We employed a photodiode to monitor the intracavity pulse build-up by a leakage of M1, as shown in Figure 6(a). The normalized output pulse is depicted in red. Notably, no perturbing pulses were detected by the oscilloscope,

indicating a precise temporal delay between the seed pulse train and the PC for the cavity length. The pulses obtained a gain of approximately 1.3 per roundtrip. In addition, the pulse-to-pulse interval was measured as 17 ns, which was consistent with the cavity length. The output pulse trains from 0.5 to 1 MHz in steps of 0.25 MHz depicted the steady temporal characteristics at the maximum output power, as shown in Figure 6(b). An oscilloscope measurement revealed a coefficient of variation (CV, the ratio of the standard deviation to the mean) lower than 1% for the pulse train at different repetition rates.

The measured intensity autocorrelation curves of the seed pulse and the output laser at 154 W are shown in Figure 7(a). The pulse width obtained through sech^2 fitting was 6.82 ps, which is similar to the pulse width of the seed laser. Figure 7(b) shows the normalized spectra of the seed laser and the 154 W amplified laser by a spectrum analyzer (AQ6370D, Yokogawa) with a span of 5 nm and 1000 points. The seed laser spectrum exhibits an FWHM of 0.380 nm, centered at 1030.78 nm, corresponding to a pulse duration of 2.9 ps at the transform limit. The spectrum at 154 W had an FWHM of 0.486 nm and was centered at 1030.78 nm,
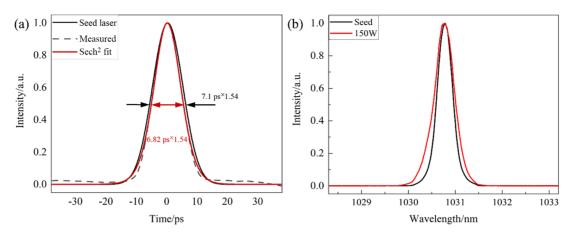
Figure 7. (a) Measured autocorrelation traces of the amplified pulses. (b) Optical spectrum of the amplifier.
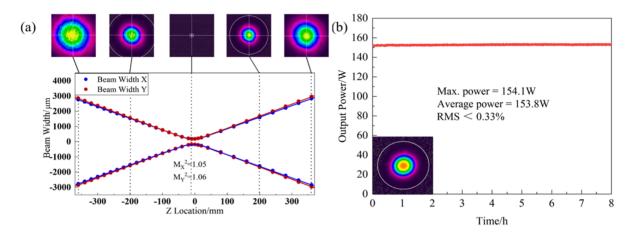

Figure 8. (a) Beam quality of the laser at 154.1 W. (b) Power stability of the laser at 154.1 W.

corresponding to a pulse duration of 2.3 ps at the transform limit. Notably, no significant shift of spectrum center is observed after amplification. During the amplification phase, the spectrum FWHM exhibited a slight broadening, and the pulse width experienced a slight compression. These phenomena could be attributed to the non-linear effects, such as self-phase modulation, which arose at high power. Moreover, the multiple roundtrips within the cavity introduced chirps, leading to a deviation of the pulse width from the transform-limited pulse duration.

We measured the beam quality of the output power at 154.1 W with a repetition rate of 1 MHz, using a beam quality analyzer (Beamsquare SP90440, Ophir). The beam quality factors are $M_X^2 = 1.05$ and $M_Y^2 = 1.06$, with the upper insets showing the far-field beam shapes at various positions, as shown in Figure 8(a). The beam quality is approaching the diffraction limit at 154.1 W. The far-field beam shapes indicate well-defined Gaussian profiles for the laser. In addition, we evaluated the power stability of the amplified laser at the maximum power over an 8-hour duration, as depicted in Figure 8(b). An outstanding stability was demonstrated by the average power at 153.8 W, with a fluctuation of less than 0.33% root mean square

(RMS). The laser exhibited exceptional temporal and spatial performance simultaneously, owing to its meticulous thermal management and optimized cavity design, which gives it strong potential for scientific research and industrial applications.

The TDL offers an attractive advantage in producing high-power and high-quality pulse lasers. Our thin-disk regenerative amplifier showcases excellent characteristics through a series of methods. Initially, the utilization of a top-hat ZPL at 969 nm for the pump resulted in a reduction of over one-third in wasted heat. This approach reduced wavefront distortions caused by thermal lensing, consequently minimizing diffraction losses. Subsequently, the thinness of the thin-disk, multi-pass pump system and higher gain per roundtrip would ensure sufficient gain for the seed pulses. These strategies effectively mitigated axial thermal accumulation within the crystal. Finally, a diamond heat sink and an efficient microchannel impingement cooling structure provided a high heat conductivity coefficient, and thus effectively managed excessive heating of the disk at high power. Experimental results indicated that these optimization strategies for disk regenerative amplifiers significantly improved output efficiency, beam quality and stability.

3. Conclusion

In summary, we have introduced a novel approach to achieving an efficient and high-power ultrafast laser system using a custom-designed 48-pass Yb:YAG thin-disk regenerative amplifier pumped by a ZPL 969 nm LD. The experimental results demonstrated exceptional performance, with the amplifier delivering an output power of 154 W and achieving an impressive optical-to-optical efficiency of 61%, marking the highest reported conversion efficiency in ultrafast thin-disk regenerative amplifiers to date. The measured M^2 factor of 1.06 indicates excellent beam quality, and the amplifier operates at room temperature with exceptional stability at a repetition rate of 1 MHz, exhibiting an RMS stability of less than 0.33%. Overall, this study significantly contributes to the field of laser amplification systems, particularly in terms of efficiency and power. The demonstrated Yb:YAG thin-disk regenerative amplifier holds great promise for a wide range of applications, including material processing, scientific research and laser manufacturing, where high-power and efficient laser sources are critical. This improvement marks a significant advancement in ultrafast laser technology, opening up new possibilities for practical and scientific innovations.

Acknowledgements

References

1. C. Gu, Z. Zuo, D. Luo, Z. Deng, Y. Liu, M. Hu, and W. Li, PhotoniX **1**, 7 (2020).
2. H. Wang, C. Yu, X. Wei, Z. Gao, G. Xu, D. Sun, Z. Li, Y. Zhou, Q. Li, B. Zhang, J. Xu, L. Wang, Y. Zhang, Y. Tan, and Y. Tao, J. Synchrotron Radiat. **24**, 667 (2017).
3. E. H. Penilla, L. F. Devia-Cruz, A. T. Wieg, P. Martinez-Torres, N. C. Espitia, P. Sellappan, Y. Kodera, G. Aguilar, and J. E. Garay, Science **365**, 803 (2019).
4. J. Finger and M. Reininghaus, Opt. Express **22**, 18790 (2014).
5. A. M. Rodin, M. Grishin, and A. Michailovas, Opt. Laser Technol. **76**, 46 (2016).
6. Z. Liu, J. Siegel, M. Garcia-Lechuga, T. Epicier, Y. Lefkir, S. Reynaud, M. Bugnet, F. Vocanson, J. Solis, G. Vitrant, and N. Destouches, ACS Nano **11**, 5031 (2017).
7. J. Zuo, H. Yu, S. Zou, Z. Dong, C. He, S. Xu, C. Ning, X. Chen, X. Li, and X. Lin, High Power Laser Sci. Eng. **11**, e22 (2023).
8. J. Xu, R. Su, H. Xiao, P. Zhou, and J. Hou, Chin. Opt. Lett. **10**, 031402 (2012).
9. A. Agnesi, L. Carra, P. Dallocchio, F. Pirzio, G. Reali, A. Tomaselli, D. Scarpa, and C. Vacchi, IEEE J. Quantum Electron. **44**, 952 (2008).
10. P. Russbueldt, D. Hoffmann, M. Hofer, J. Lohring, J. Luttmann, A. Meissner, J. Weitenberg, M. Traub, T. Sartorius, D. Esser, R. Wester, P. Loosen, and R. Poprawe, IEEE J. Select. Top. Quantum Electron. **21**, 3100117 (2015).
11. A. Loescher, F. Bienert, C. Roecker, T. Graf, M. Gorjan, J. A. Der Au, and M. A. Ahmed, Opt. Continuum **1**, 747 (2022).
12. F. Saltarelli, A. Diebold, I. J. Graumann, C. R. Phillips, and U. Keller, Optica **5**, 1603 (2018).
13. Y. Gao, S. Xu, Y. Chen, M. Liu, D. Ouyang, X. Wu, J. Chen, J. Zhao, C. Guo, X. Liu, Q. Lue, and S. Ruan, Acta Photon. Sin. **53**, 0214002 (2024).
14. J. Zuo and X. Lin, Laser Photon. Rev. **16**, 2270025 (2022).
15. T. Dietz, M. Jenne, D. Bauer, M. Scharun, D. Sutter, and A. Killi, Opt. Express **28**, 11415 (2020).
16. J. Negel, A. Loescher, A. Voss, D. Bauer, D. Sutter, A. Killi, M. A. Ahmed, and T. Graf, Opt. Express **23**, 21064 (2015).
17. C. Herkommer, P. Krötz, R. Jung, S. Klingebiel, C. Wandt, R. Bessing, P. Walch, T. Produit, K. Michel, D. Bauer, R. Kienberger, and T. Metzger, Opt. Express **28**, 30164 (2020).
18. C. Honninger, I. Johannsen, M. Moser, G. Zhang, A. Giesen, and U. Keller, Appl. Phys. B Lasers Opt. **65**, 423 (1997).
19. C. Li, R. Liu, F. Gong, Y. Jia, S. Deng, Y. Jin, and G. Li, Optik **130**, 511 (2017).
20. M. Smrz, J. Muzik, M. Chyla, S. S. Nagisetty, P. Sikocinski, O. Novák, and T. Mocek, in *EUV Source Workshop* (2019), p. 20.
21. A. Alabbadi, M. Larionov, and F. Fink, Opt. Lett. **47**, 202 (2022).
22. M. Smrz, J. Muzik, D. Stepankova, H. Turcicova, O. Novak, M. Chyla, P. Hauschwitz, J. Brajer, J. Kubat, F. Todorov, and T. Mocek, OSA Continuum **4**, 940 (2021).
23. W. Christoph, H. Clemens, J. Robert, K. Sandro, K. Peter, R. Michael, Y. T. Catherine, M. Knut, and M. Thomas, in *22nd International Conference on Ultrafast Phenomena*, Optica Publishing Group. (Academic, Washington, DC, USA, 2020), paper HM2B.4.
24. T. Metzger, A. Schwarz, C. Y. Teisset, D. Sutter, A. Killi, R. Kienberger, and F. Krausz, Opt. Lett. **34**, 14 (2009).
25. R. Jung, J. Tuemmler, and I. Will, Opt. Express **24**, 883 (2016).
26. J. Dong, H. T. Chen, H. L. Wang, X. S. Jia, G. Z. Zhu, A. Kozlov, and X. Zhu, Acta Opt. Sin. **41**, 1414003 (2021).
27. J. Guo, Z. Gao, D. Sun, X. Du, Y. Gao, and X. Liang, High Power Laser Sci. Eng. **10**, e2 (2022).
28. M. Michael, B. Aleksander, K. Max, and S. Dirk, in *International Congress on Applications of Lasers and Electro-Optics*, the Laser Institute of America. (Academic, Orlando, FL, USA, 2015), p. 218.
29. C. Chang, P. Krogen, H. Liang, G. J. Stein, J. Moses, C. Lai, J. P. Siqueira, L. E. Zapata, F. X. Kaertner, and K. Hong, Opt. Lett. **40**, 665 (2015).
30. S. Radmard, A. Moshaii, and K. Pasandideh, Sci. Rep. **12**, 16918 (2022).
31. M. Saravani, A. F. M. Jafarnia, and M. Azizi, Opt. Laser Technol. **44**, 756 (2012).
32. B. Weichelt, A. Voss, M. A. Ahmed, and T. Graf, Opt. Lett. **37**, 3045 (2012).
33. S. Piehler, B. Weichelt, A. Voss, M. A. Ahmed, and T. Graf, Opt. Lett. **37**, 5033 (2012).